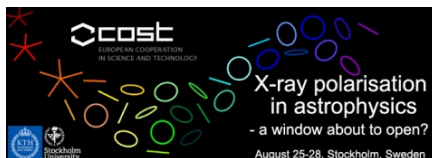


# PROBING MAGNETAR MAGNETOSPHERE THROUGH X-RAY POLARIZATION MEASUREMENTS

**Roberto Taverna**

Dept. of Physics and Astronomy – University of Padova

in collaboration with: Roberto Turolla, Fabio Muleri, Paolo Soffitta,  
Sergio Fabiani, Luciano Nobili, Enrico Costa



X-ray polarisation in astrophysics - a window about to open?  
Stockholm, August 25<sup>th</sup> – 28<sup>th</sup>, 2014

# Outline

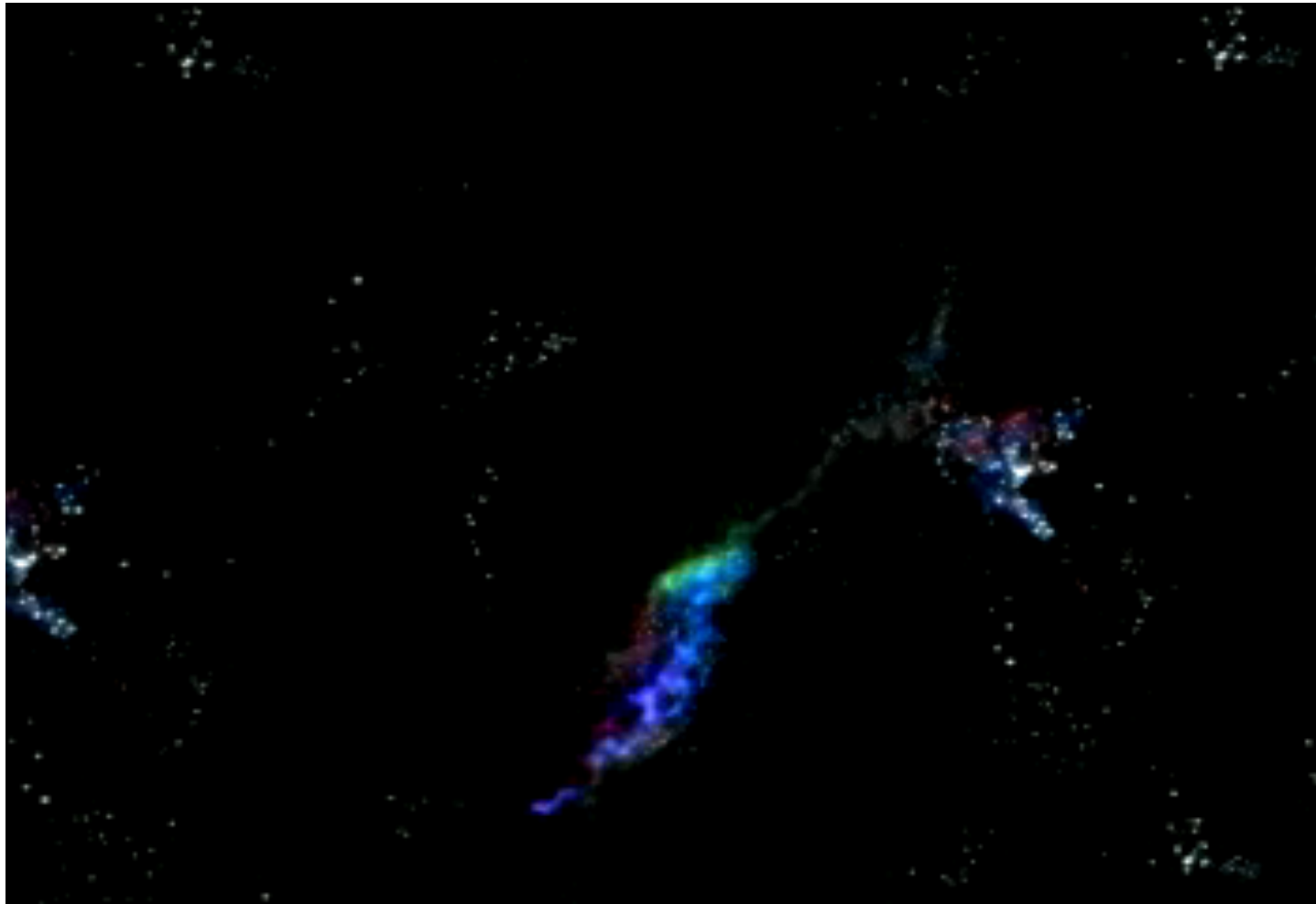
- Introduction
- Polarization
- Simulations
- Observational perspectives

## Why to study polarization of magnetars emission?

- Theoretical simulations based on Resonant Cyclotron Scattering (RCS) show that spectra may be indistinguishable even if magnetospheric parameters are quite different
- X-ray polarimetry on the radiation emitted by a magnetar can resolve the physical features and geometrical configuration of the magnetosphere
- Polarization measurements are sensitive to Quantum Electro-Dynamics (QED) effects which are predicted by the theory and can prove the existence of ultra-strong fields

# Introduction

# Discovery of magnetars



[www.nasa-usa.de](http://www.nasa-usa.de)

# Magnetars - Basics

- Magnetars are isolated Neutron Stars powered by their own magnetic energy, observationally identified with SGRs and AXPs

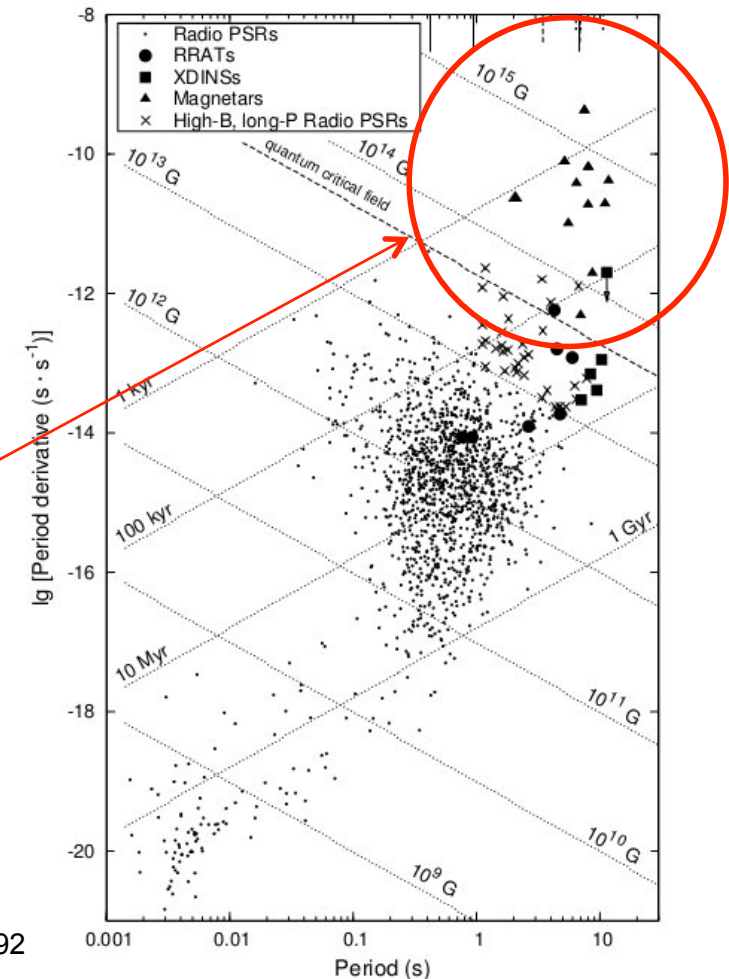
$$- L > \dot{E}$$

$$- B \gtrsim B_q \text{ (at least inside the star)}$$

$$B = 3.2 \times 10^{19} \sqrt{P\dot{P}} \text{ G}$$

$$B \sim 10^{14} \text{ G}$$

Kondratiev, V.I. et al 2009, ApJ 702, 692



# Magnetars - Basics

- Magnetars are isolated Neutron Stars powered by their own magnetic energy, observationally identified with SGRs and AXPs

- $L > \dot{E}$

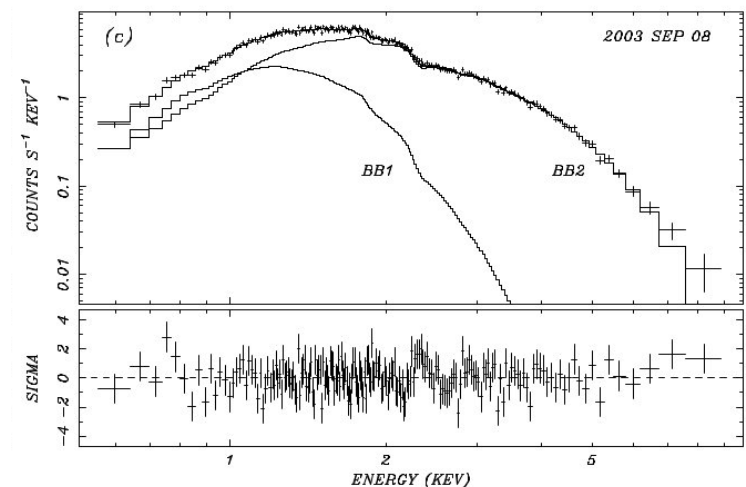
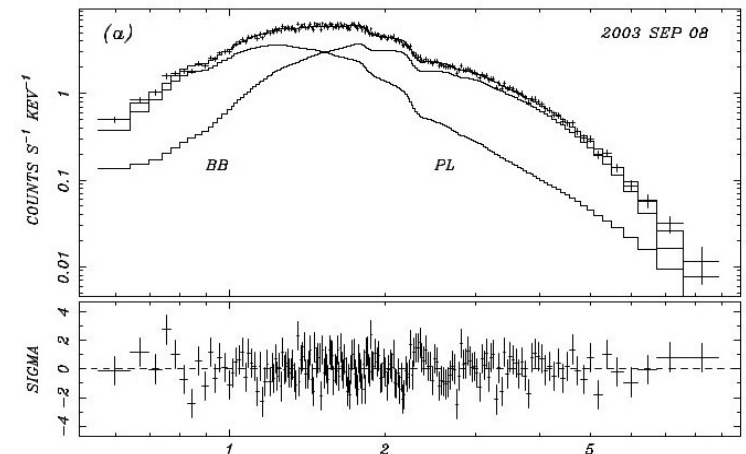
- $B \gtrsim B_q$  (at least inside the star)

- Persistent emission

- X-rays in the range  $\sim 0.2 - 10$  keV

- $L \sim 10^{31} - 10^{36}$  erg/s

- Spectrum: BB + PL (or BB + BB)



Mereghetti S. 2008, A&A, REV 15, 225

# Magnetars - Basics

## • Bursting activity

- Giant flares

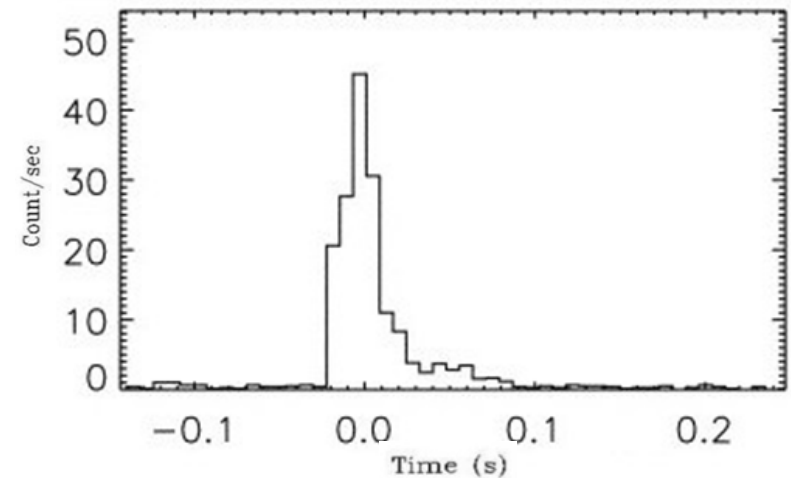
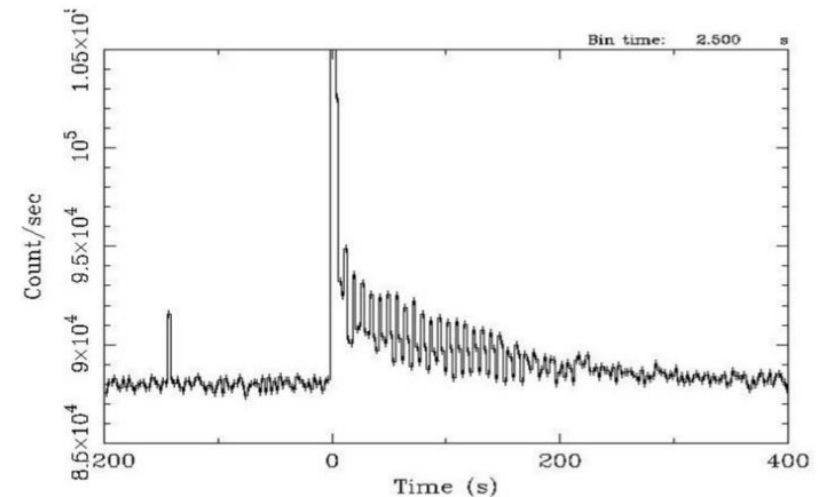
$$\Delta t_{\text{spike}} \sim 10 \text{ s} - \Delta t_{\text{tail}} \sim 10^2 \text{ s}$$

$$L = 10^{44} - 10^{47} \text{ erg/s}$$

- Short bursts

$$\Delta t \sim 0.1 - 1 \text{ s}$$

$$L \sim 10^{38} - 10^{41} \text{ erg/s}$$

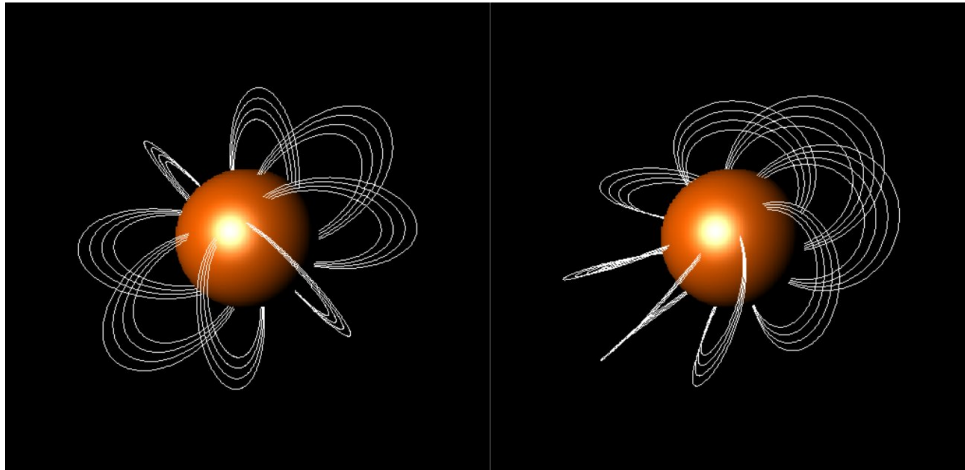


Mereghetti S. 2008, A&A, REV 15, 225



# Theoretical magnetar model

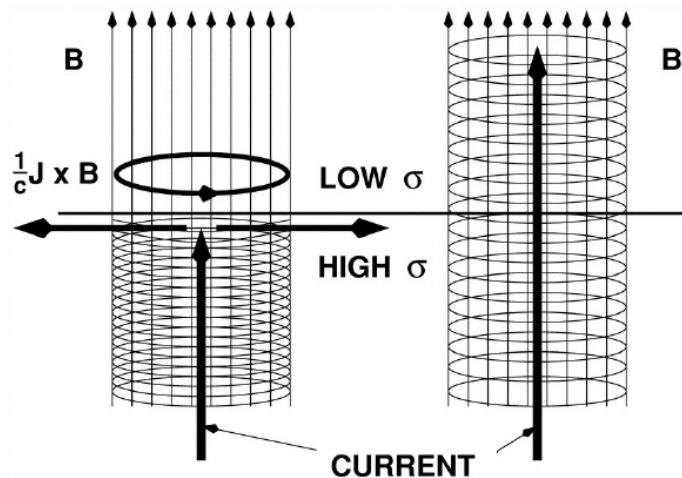
## Twist of the external magnetic field



Courtesy of Roberto Turolla

Twist angle:

$$\Delta\phi_{N-S} = 2 \lim_{\theta \rightarrow 0} \int_{\theta}^{\pi/2} \frac{B_{\phi}}{\sin \theta B_{\theta}} d\theta$$



Giant flares and short bursts are related to starquakes induced by the magnetic stresses or by magnetic reconnection in the magnetosphere

Thompson, Lyutikov & Kulkarni, 2002 ApJ, 574: 332-355

# Resonant Cyclotron Scattering

- A non-potential magnetic field implies that charged particles must flow along the closed magnetic field lines
- Thermal photons are resonantly scattered by moving electrons in the magnetosphere

$$\hbar\omega = \frac{\hbar\omega_B}{\gamma(1 - \beta \cos \theta_{Bk})}$$

- For typical values of parameters, scattering occurs within a radius

$$r_{esc} \sim 10 R_{NS}$$

# Polarization

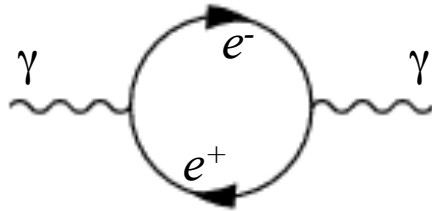
# Polarization of magnetar emitted radiation

- 

$$B = 3.2 \times 10^{19} \sqrt{P \dot{P}} \text{ G}$$

$$B \sim 10^{14} \text{ G}$$

# Vacuum polarization effects



Component  
in the wave  
magnetized

- Writing down the wave equation system for the components of electric field associated to each

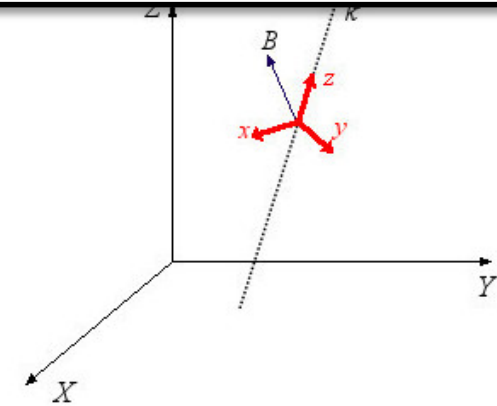
$$\frac{dQ}{dz} = -2PV$$

$$\frac{dU}{dz} = -(N - M)V$$

$$\frac{dV}{dz} = 2PQ + (N - M)U$$

$$\frac{\partial A_x}{\partial z} = \frac{ik_0 \delta}{2} [MA_x + PA_y]$$

$$\frac{\partial A_y}{\partial z} = \frac{ik_0 \delta}{2} [PA_x + NA_y]$$



## Vacuum polarization effects

- Comparing the scale lengths

$$\ell_A \sim \frac{1}{k_0 \delta} \propto B^{-2} \quad \text{and} \quad \ell_B \sim \frac{B}{|\hat{k} \cdot \nabla B|}$$

it can be seen that photons propagate in vacuo through two different regions:

- **adiabatic region**, where the polarization mode is not changed; it can reach a distance  $\sim 150 R_{NS}$  from the star
- **external region**, where the direction of the electric field freezes and the polarization mode varies

# Simulations

# Simplifications

- Despite the fact that the twist is more likely localized into bundles of field lines, we considered the magnetosphere as globally twisted
- Motion of the electrons along the closed field lines as superposition of a bulk motion (velocity  $\beta$ ) and a 1D maxwellian (temperature  $T_{el}$ )
- Seed photons are assumed 100% polarized in the X-mode

$$\kappa_X \sim \kappa_O \left( \frac{\omega}{\omega_B} \right)^2$$

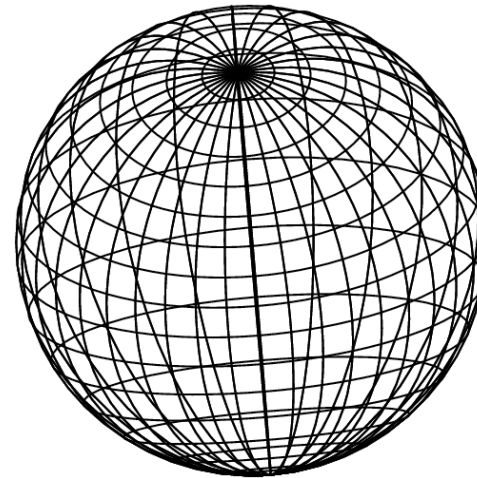
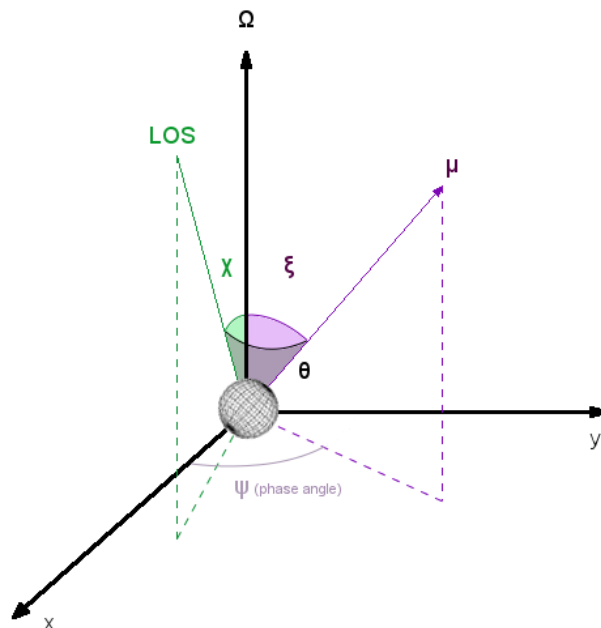


## Numerical implementation

- Monte Carlo code developed by Nobili, Turolla & Zane (2008) with the addition of a specific routine for QED effects
  - Input parameters:  $B_p$ ,  $\Delta\phi_{N-S}$ ,  $\beta$  and  $T_{e1}$
  - Output quantities: spectrum,  $\chi_{pol}$ ,  $\Pi_L$  and  $\Pi_C$  (obtained by combinations of the Stokes parameters)
- Both phase-averaged (over the azimuthal angle) and phase-resolved simulations were performed
- The expected degree of polarization for phase-resolved measurements is greater than for phase-averaged ones

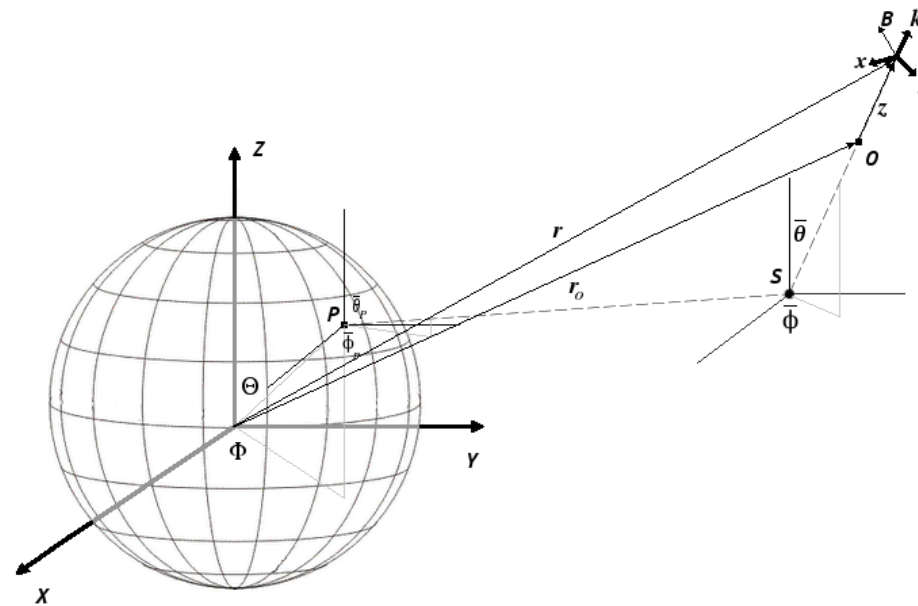
# Geometry

- Orientation angles
  - $\chi$  = angle between  $\hat{\Omega}$  and LOS -  $\xi$  = angle between  $\hat{\Omega}$  and  $\hat{\mu}$
$$\cos \theta = \cos \chi \cos \xi + \sin \chi \sin \xi \cos \psi$$
  - At fixed  $\chi$  and  $\xi$ , regions of the star at different magnetic colatitudes enter into view when phase changes



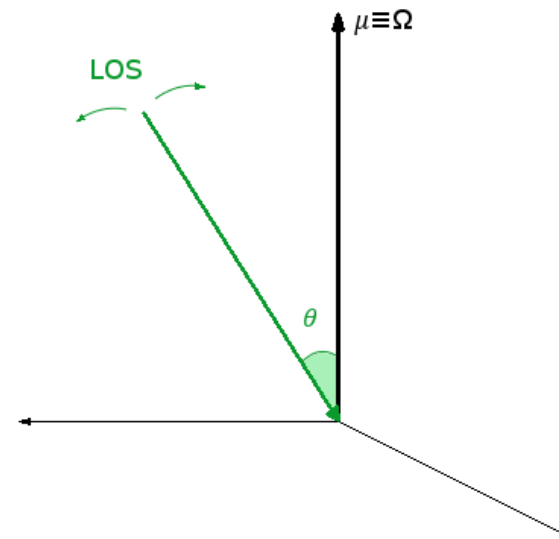
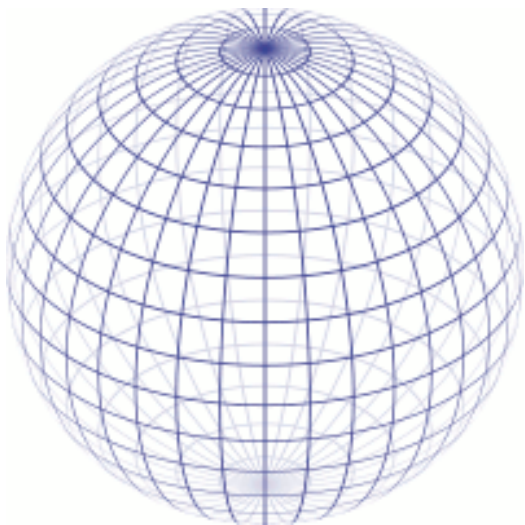
# Numerical implementation - I

Monte Carlo code developed by Nobili, Turolla & Zane (2008) follows the evolution of photons emitted by the star surface as they propagate through the magnetosphere

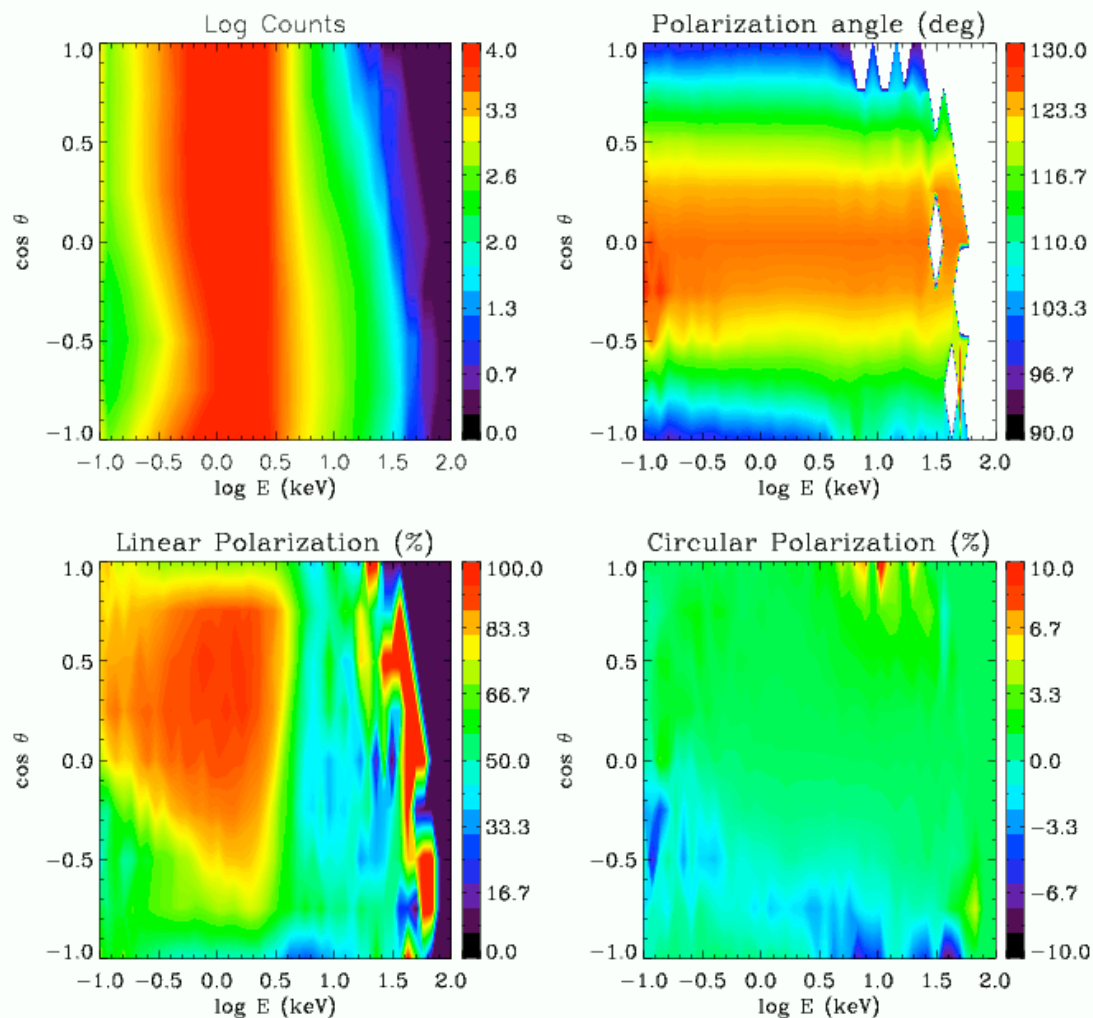


# Phase-averaged simulations - Geometry

- Phase-averaged simulations
  - Star is assumed to be an aligned rotator ( $\hat{\mu} \equiv \hat{\Omega}$ )
  - $\theta$  is the angle between  $\hat{\mu}$  and LOS
  - Data are averaged over the azimuthal angle  $\Phi$



# Phase-averaged simulations – Various $B_p$

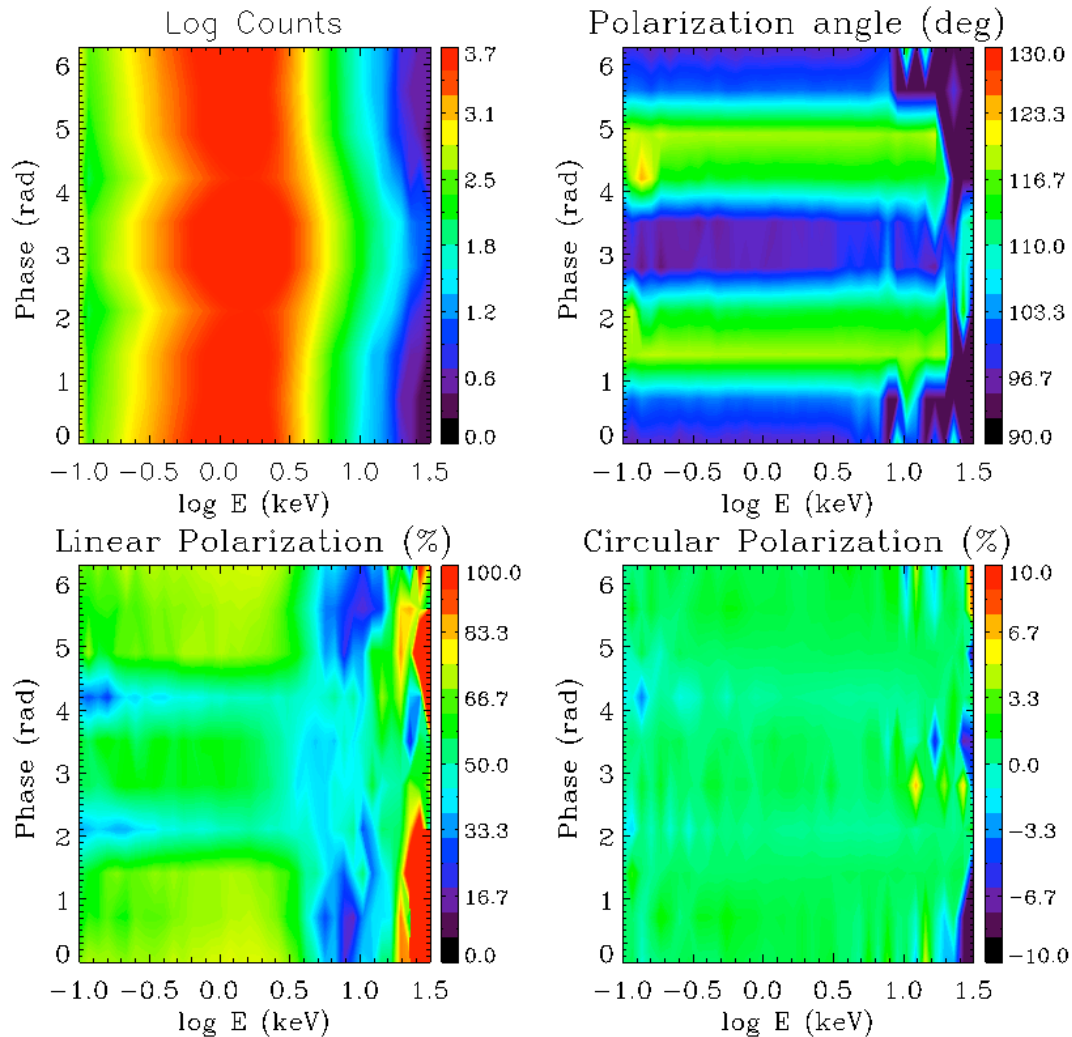


$$B_p = 5 \times 10^{12} - 1 \times 10^{15} \text{ G}$$

- Only spectrum and linear polarization fraction are substantially modified by the variation of  $B_p$
- Polarization angle and circular polarization fraction are almost unchanged

$$B_p = 5 \times 10^{12} \text{ G}$$

# Response to the variation of input parameters



Polarization observables are more sensitive to  $\Delta\phi_{N-S}$  and  $\beta$  variations

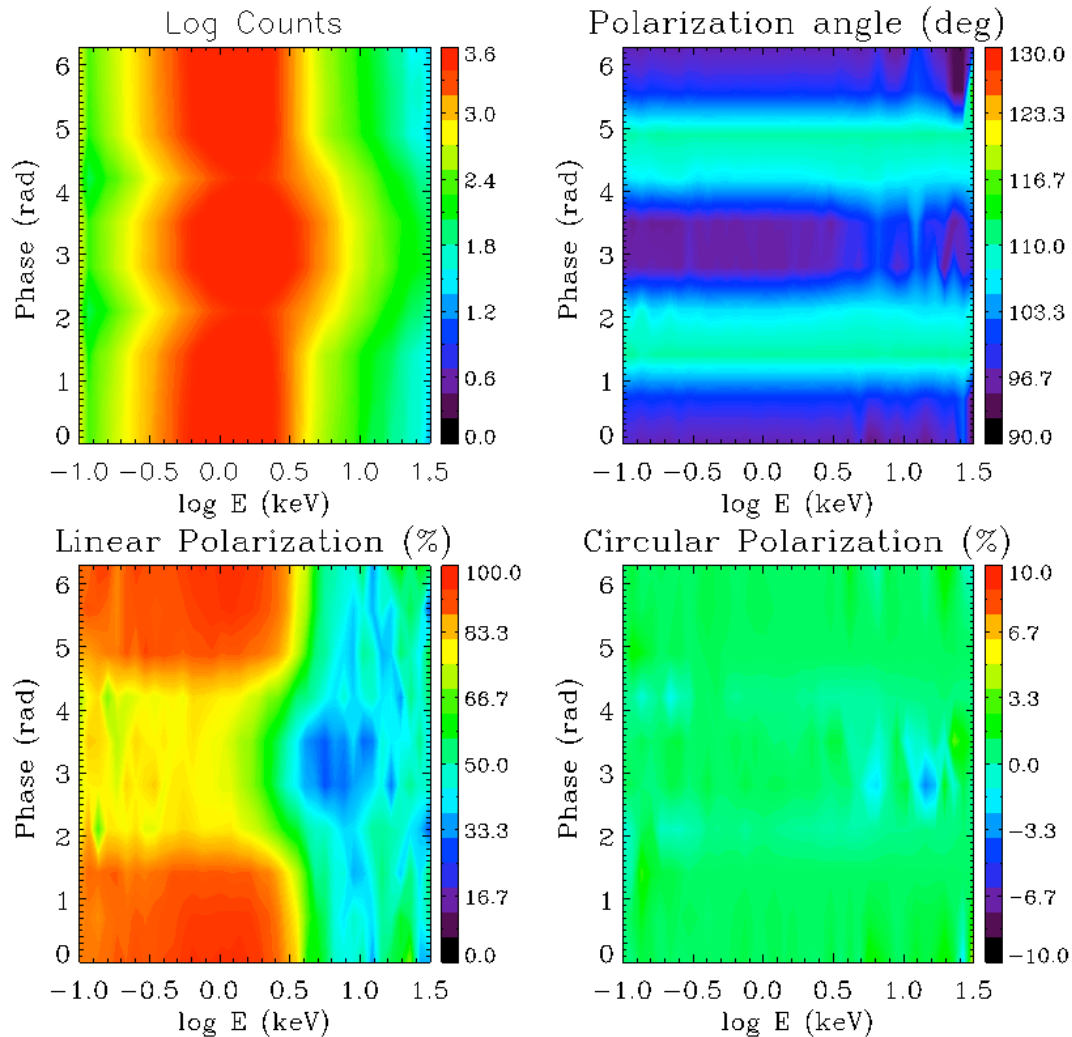
By varying  $\beta$  the most important changes affect  $\Pi_L$  ( $n_e \sim |\beta|^{-1}$ ), whereas  $\chi_{pol}$  is almost unchanged

$$\beta = 0.20$$

$$\Delta\phi = 1.0 r$$



# Response to the variation of input parameters



Polarization observables are more sensitive to  $\Delta\phi_{N-S}$  and  $\beta$  variations

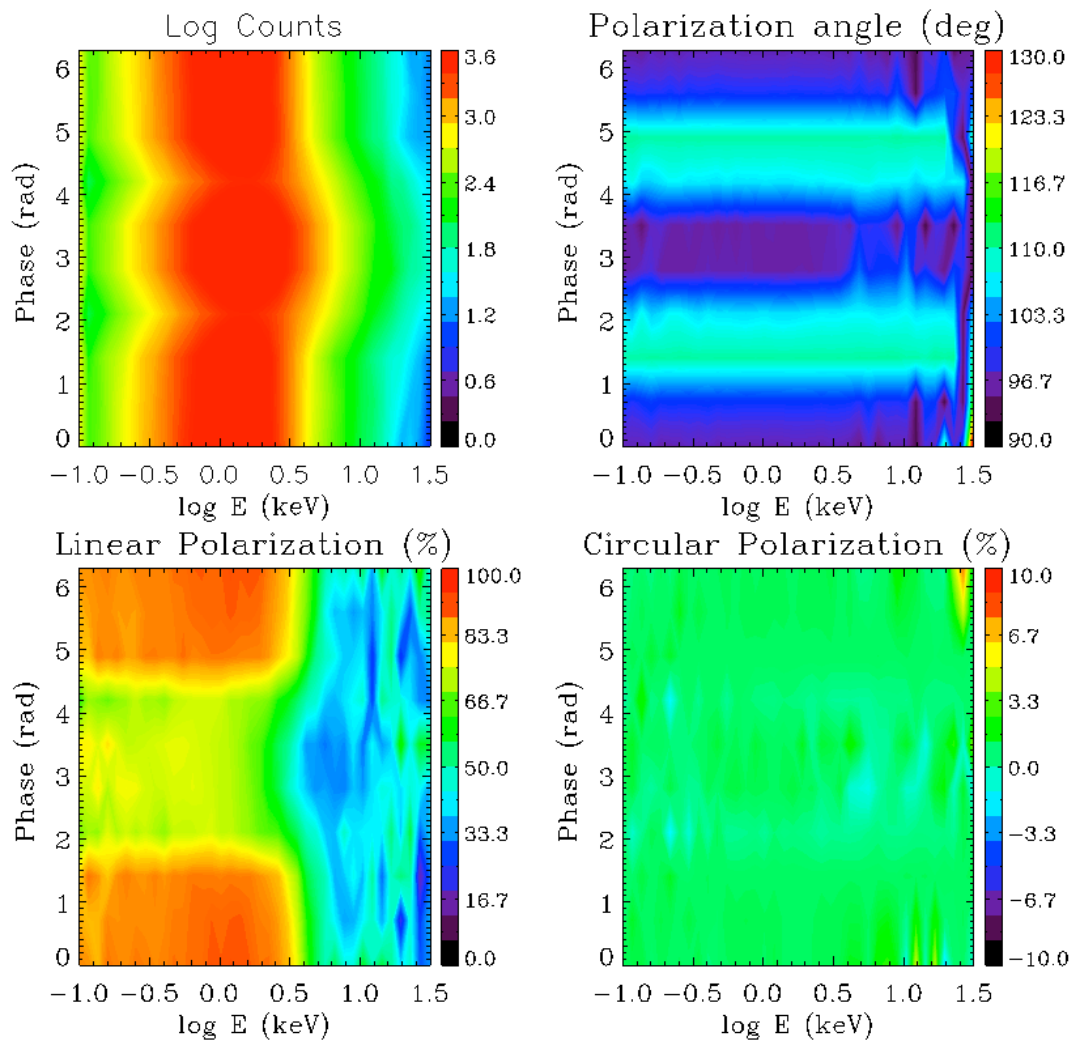
By varying  $\beta$  the most important changes affect  $\Pi_L$  ( $n_e \sim |\beta|^{-1}$ ), whereas  $\chi_{pol}$  is almost unchanged

Changing  $\Delta\phi_{N-S}$  (geometry of the magnetosphere) both  $\chi_{pol}$  and  $\Pi_L$  vary

$$\beta = 0.50$$

$$\Delta\phi = 0.7 r$$

# Polarization and spectral degeneracy removal



Particular phase resolved simulation at values of  $\beta$  and  $\Delta\phi_{N-S}$  in such a way to have the same spectra

Spectral analysis alone cannot give any information about the magnetospheric parameters

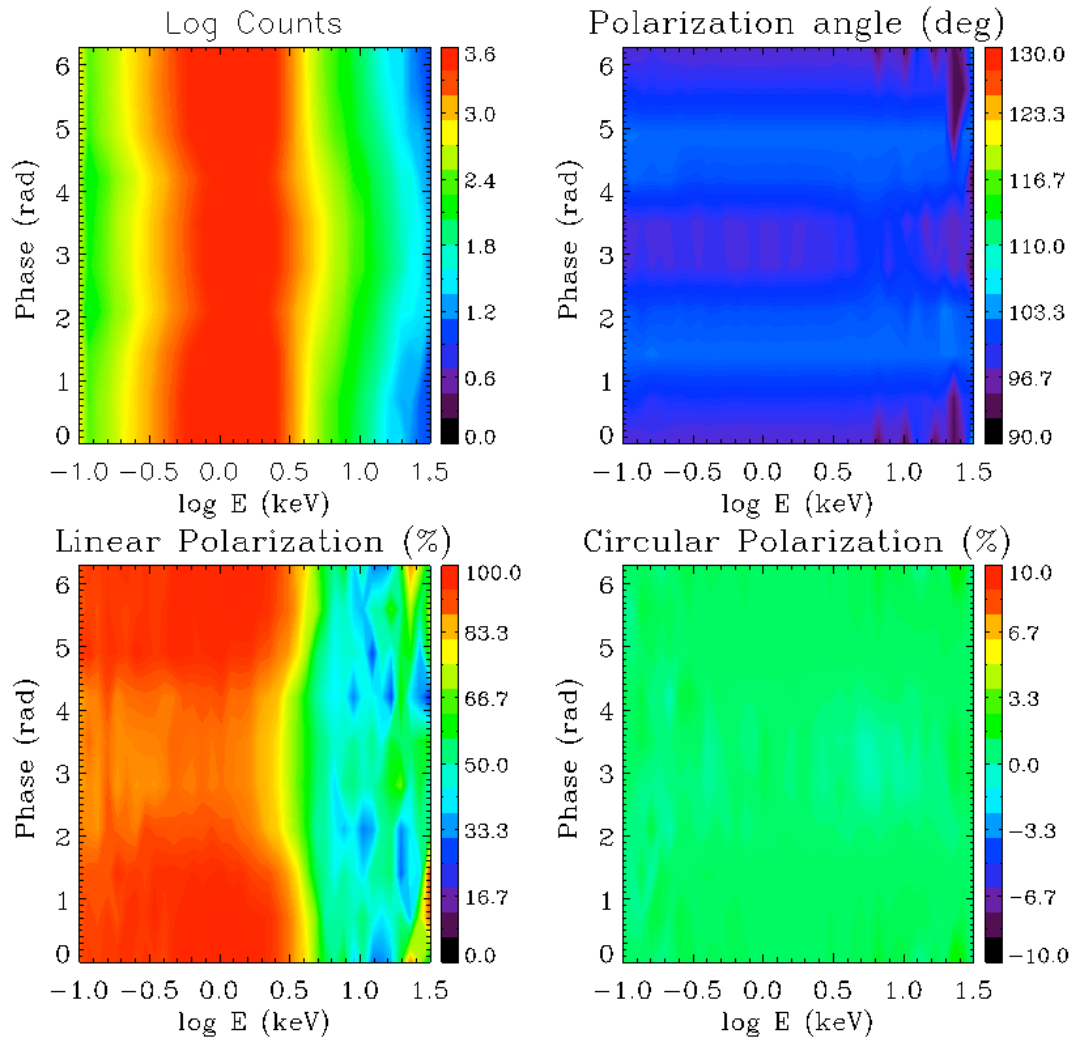
Only by studying the polarization observables it is possible to distinguish the two different cases

$$\beta = 0.40$$

$$\Delta\phi = 0.7 r$$



# Resolution of geometry from polarization observables

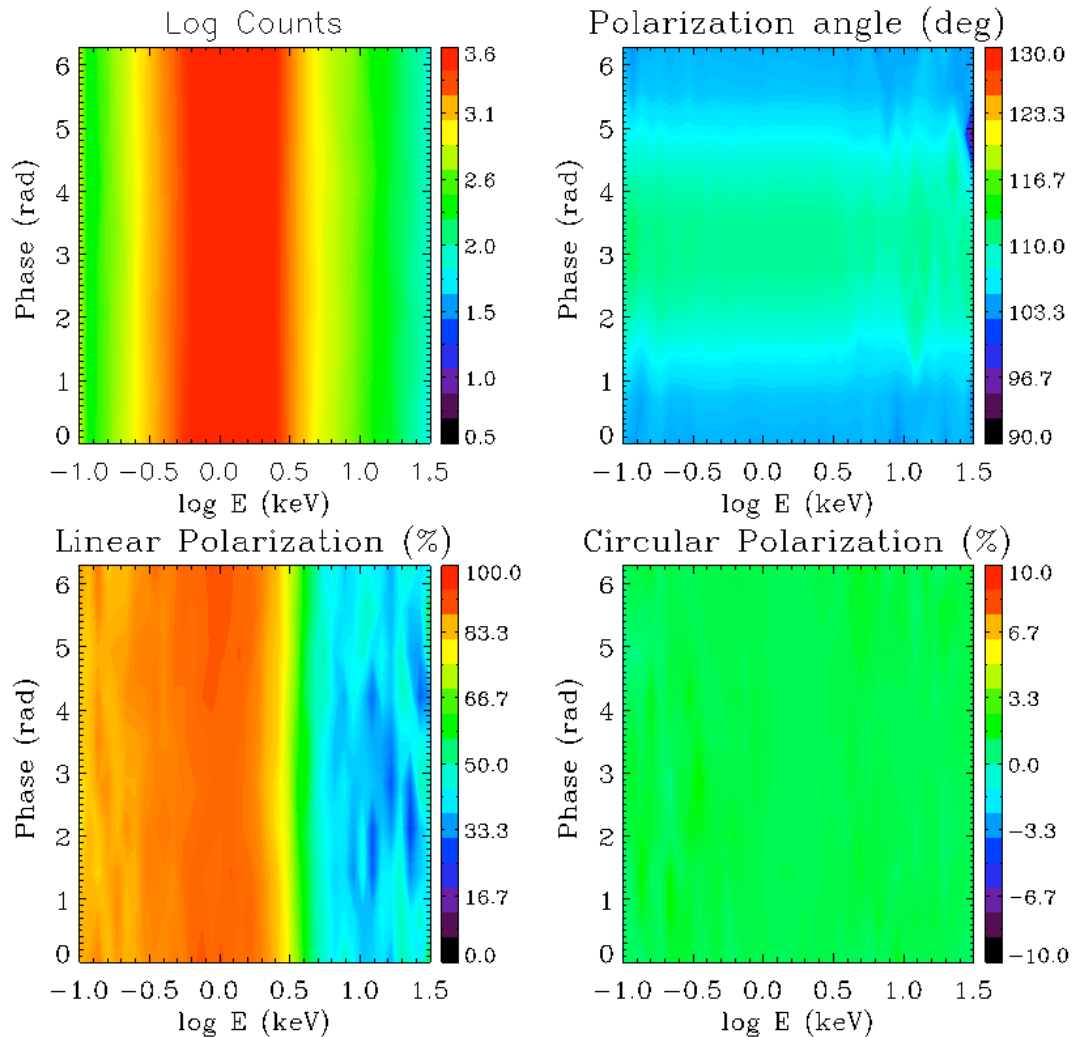


$$\Delta\phi_{N-S} = 0.3 \text{ rad}$$

Polarization observables are also sensitive to the geometry of view

In particular the absolute value of the maxima in the  $\chi_{\text{pol}}$  distribution is fixed by  $\Delta\phi_{N-S}$

# Resolution of geometry from polarization observables



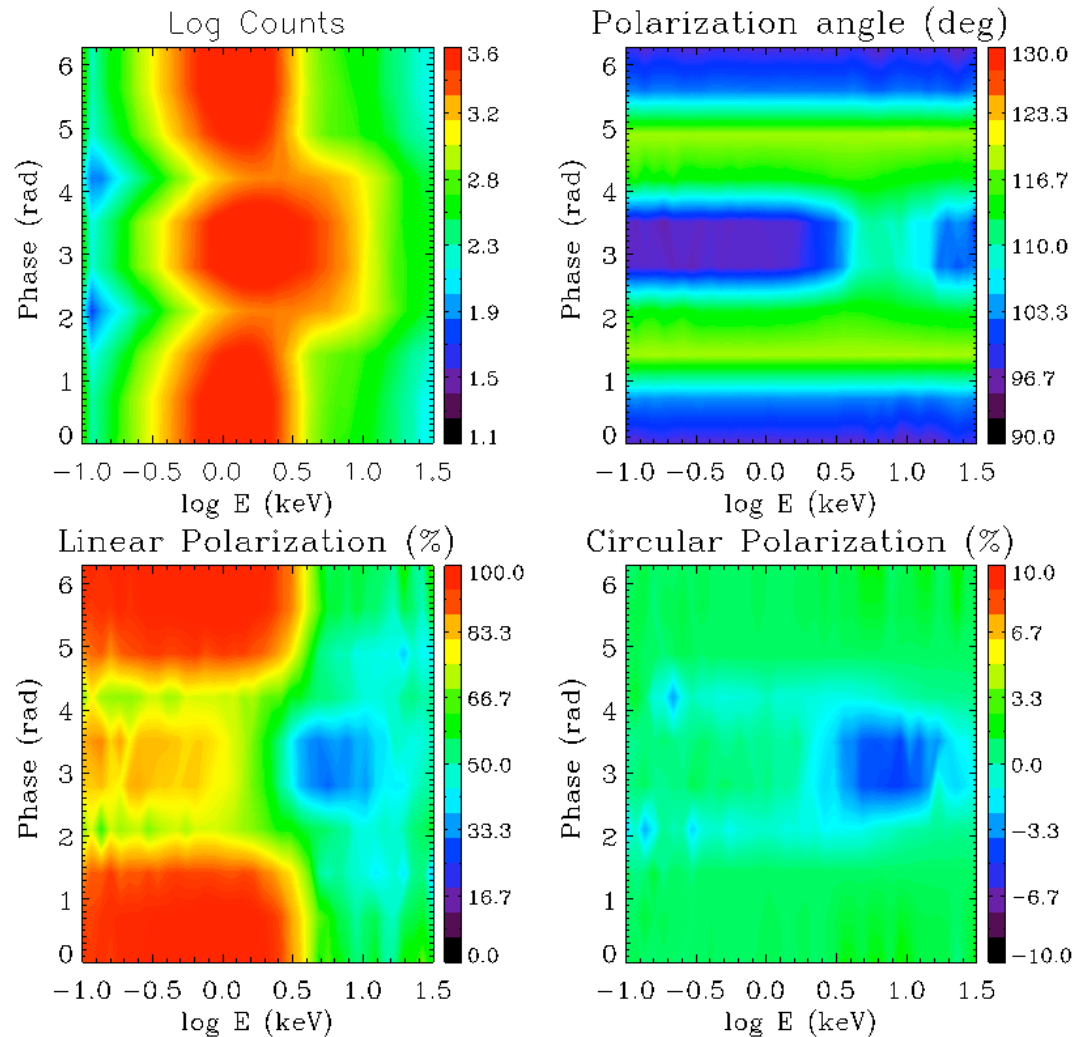
$$\chi = 45^\circ - \xi = 5^\circ$$

Polarization observables are also sensitive to the geometry of view

In particular the absolute value of the maxima in the  $\chi_{\text{pol}}$  distribution is fixed by  $\Delta\phi_{\text{N-S}}$

Instead the position of the maxima depends on the values of  $\chi$  and  $\xi$  angles

# Assessment of QED effects

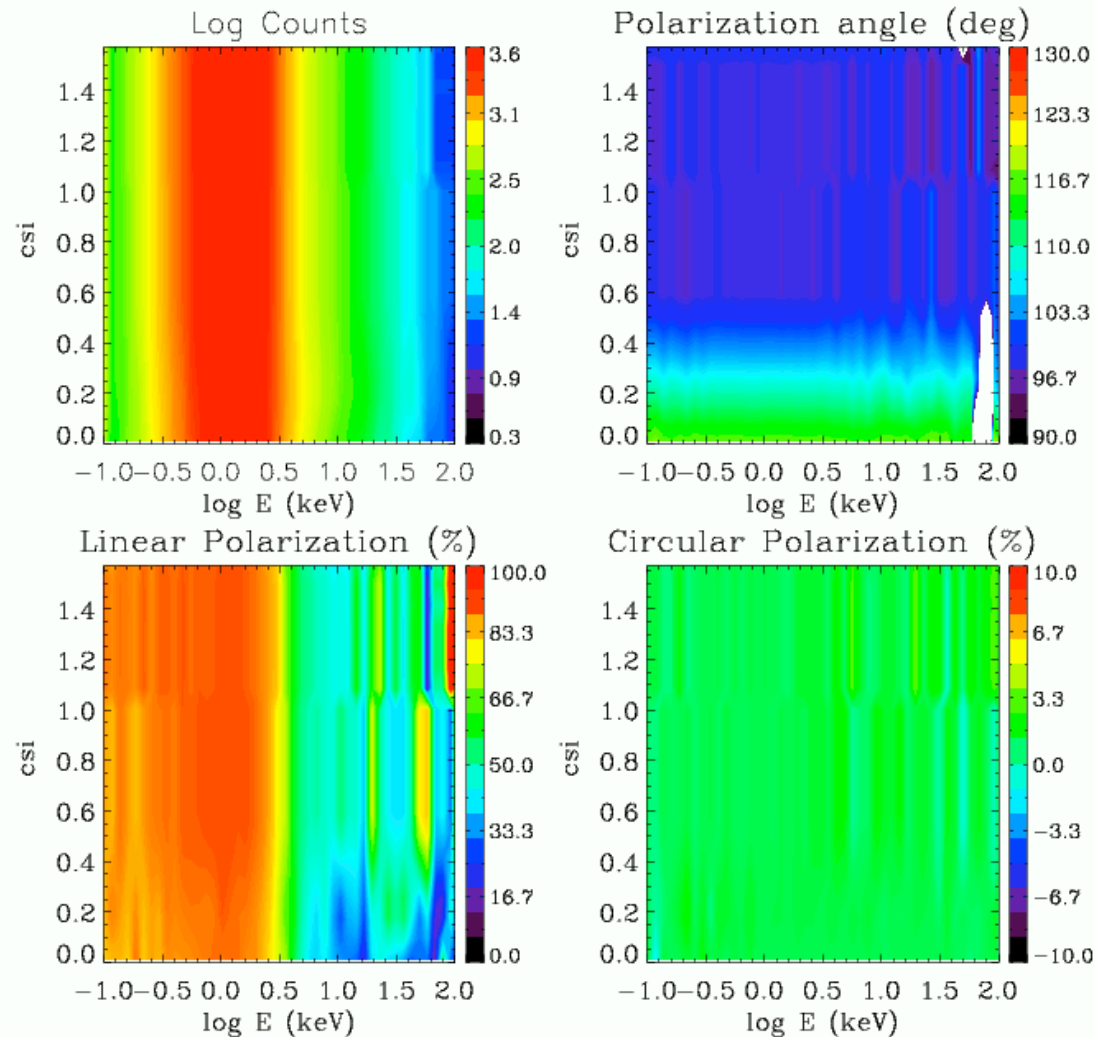


RCS + QED

Turning off the effects of magnetized vacuum, simulations appear substantially different

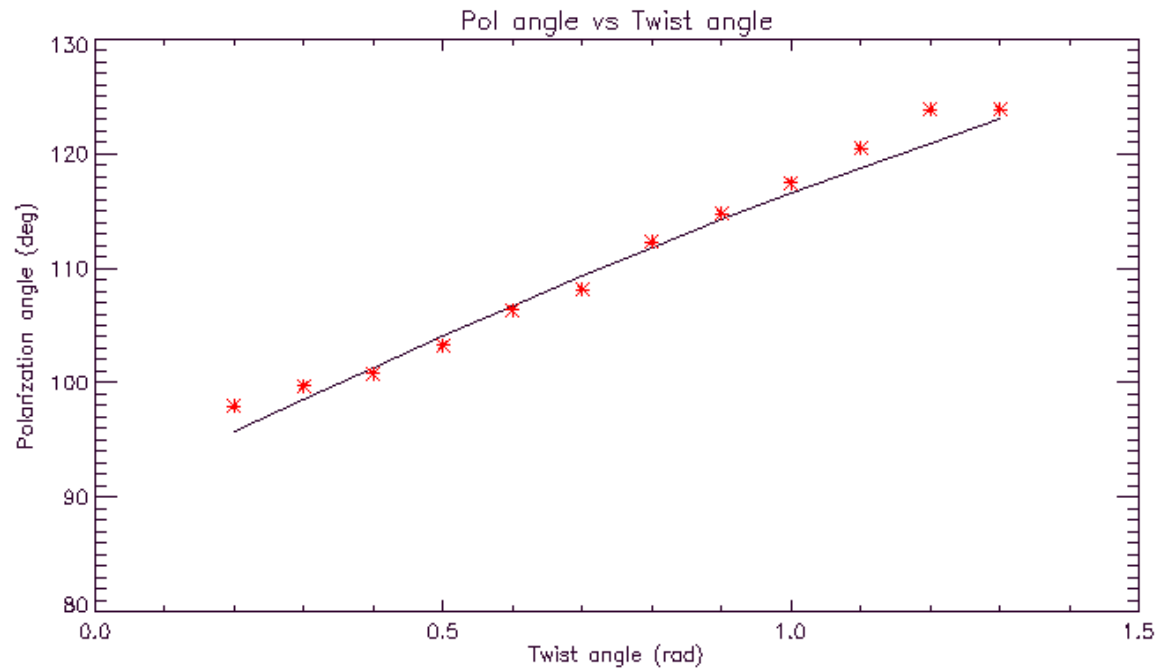
Vacuum polarization acts in smoothing out the behavior of all polarization observables

# Phase-resolved simulations – III



- Variation in phase of polarization observables and spectrum as a function of energy and  $\xi$  ( $\chi = 60^\circ$ )

# Relation between polarization angle and twist angle



Polarization and twist angles are related

$$\chi \sim \tan^{-1} \frac{B_{\phi}}{B_{\theta}} \left[ + \frac{\pi}{2} \right]$$

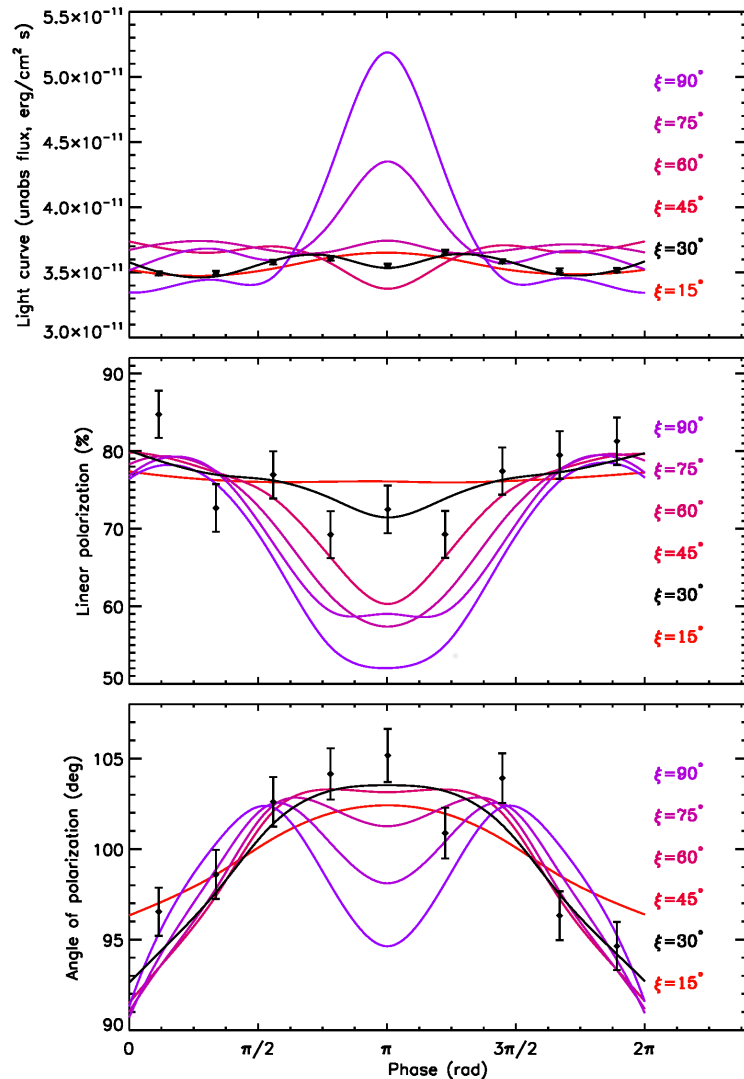
Measuring the polarization angle allows to probe the geometry of magnetars magnetospheres

# Observational perspectives

## Measuring polarization observables with XIPE

- We tried to assess the feasibility of magnetar X-ray polarization measurements using the polarimeter of the small mission XIPE, based on GPD (Soffitta et al., 2013)
- We used as a template the bright AXP 1RXS J1708 ( $\beta = 0.34$ ,  $\Delta\phi_{N-S} = 0.5$  rad,  $B_p = 4.6 \times 10^{14}$  G) with unabsorbed flux in the 2 – 6 keV range between 21 and  $35 \times 10^{-12}$  erg cm<sup>-2</sup> s<sup>-1</sup>
- Simulated data are obtained starting from the theoretical simulations and using a Monte Carlo code to produce some trial modulation curves (to simulate the response of the instrument for a total observation time of 1 Ms)

# Resolving viewing geometry



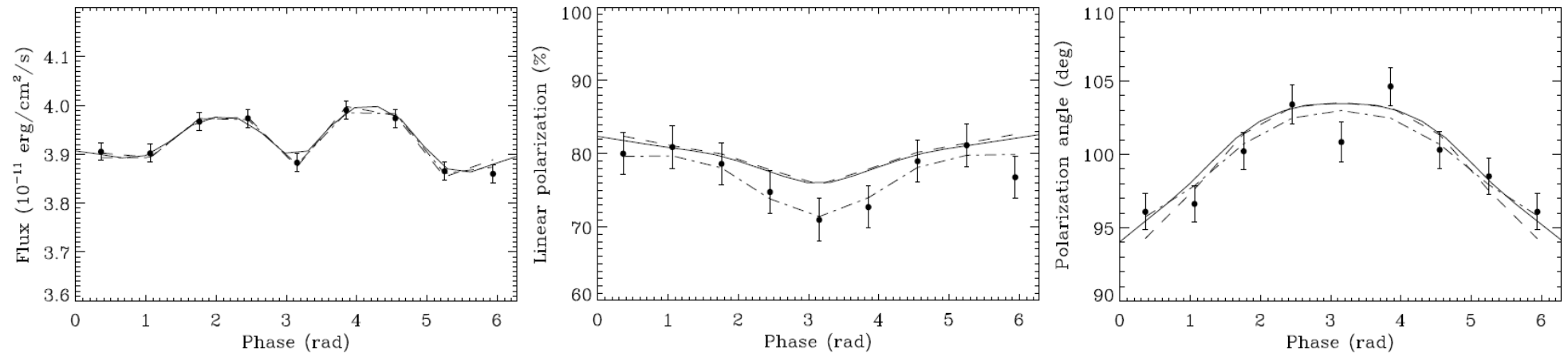
Phase-resolved simulated data (pulse profile,  $\Pi_L$  and  $\chi_{\text{pol}}$ ) in the case of the real source 1RXS J1708 for  $\chi = 60^\circ$  and  $\xi = 30^\circ$  (filled circles with error bars)

Solid lines are the theoretical models for the same values of parameters and varying  $\xi$  (the black line is the model from which measurements are taken)

Comparing theoretical models and simulated data for the polarization observables allows to know the viewing geometry



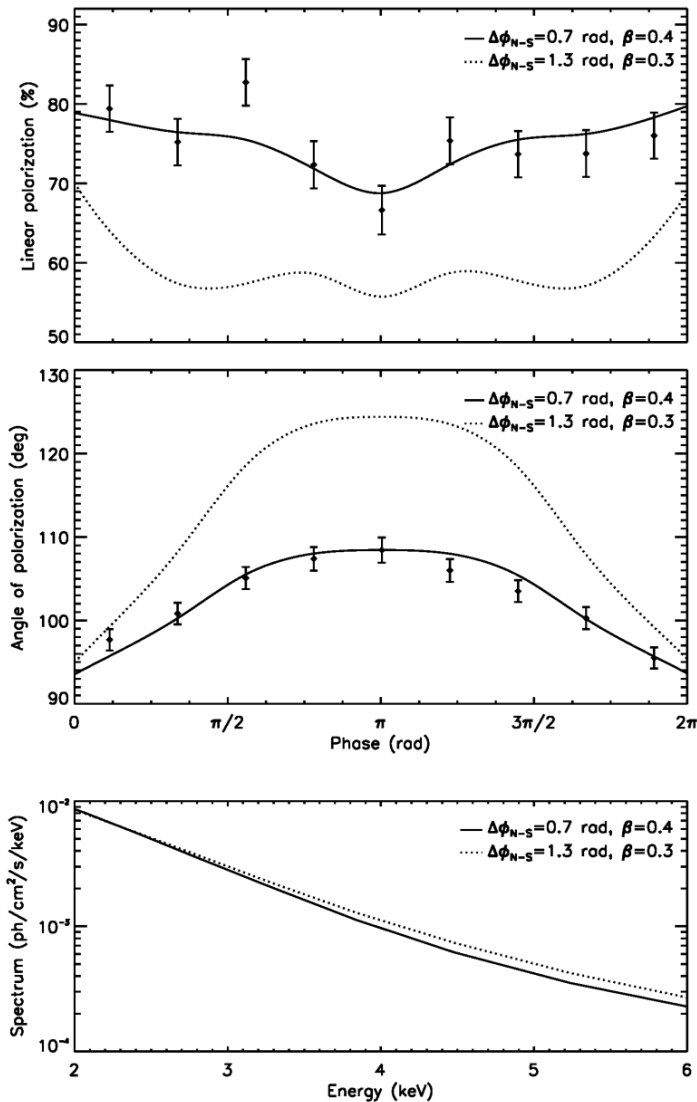
# Polarization measurements with XIPE polarimeter



	$\beta$	$\Delta\phi_{N-S}$ (rad)	$\chi$ (deg)	$\xi$ (deg)	$\chi^2_{\text{red}}$
Input val.	0.34	0.5	60	30	—
Fit val.	$0.34 \pm 0.004$	$0.51 \pm 0.01$	$61.4 \pm 0.9$	$25.7 \pm 1.8$	0.97

- Simultaneous fit of all the simulated data distributions (starting from an archive containing models with different values of the parameters)
- The result of the fit recovers with reasonable accuracy the input parameters

# Removing spectral degeneracy



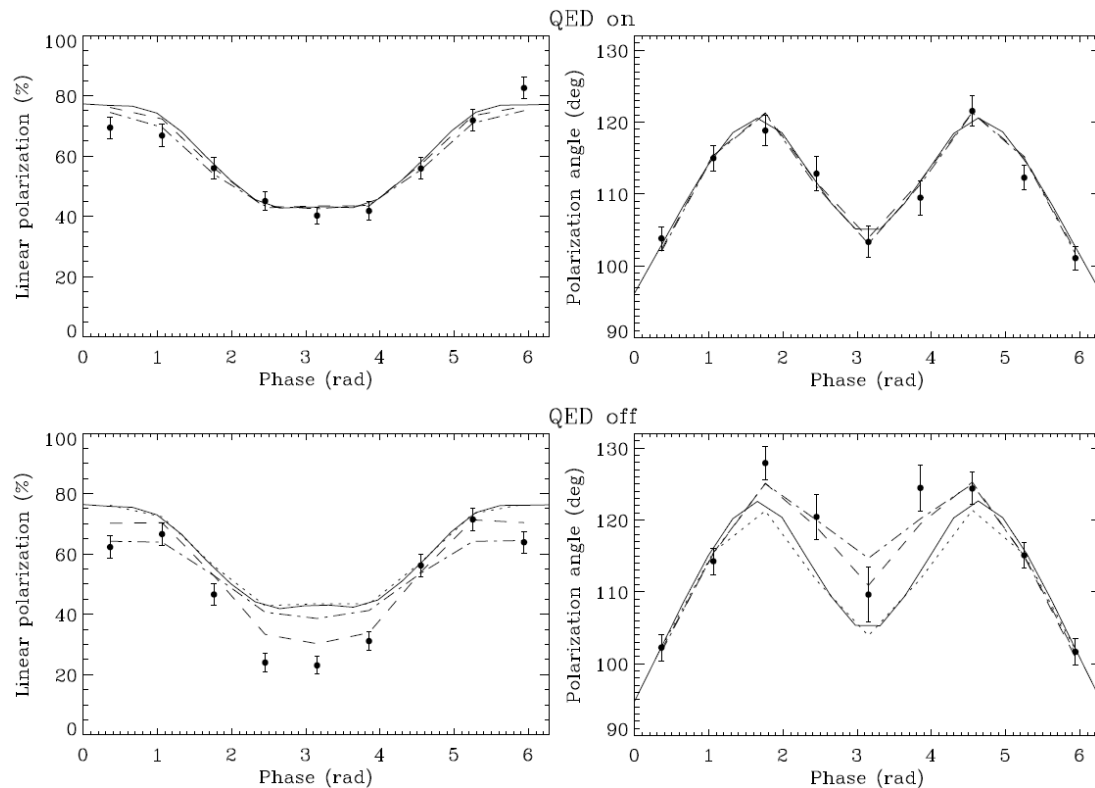
Phase-resolved  $\Pi_L$ ,  $\chi_{\text{pol}}$  and spectrum for two set of input parameters for which spectra are almost identical

Lines represent the theoretical models for  $\beta = 0.4$  and  $\Delta\phi_{N-S} = 0.7$  (solid) and  $\beta = 0.3$  and  $\Delta\phi_{N-S} = 1.3$  (dotted)

Filled circles with error bars are the simulated data generated from one of the two models (solid line one)

The comparison between models and polarization measurements unequivocally distinguish the two cases

# Revealing the effects of vacuum polarization

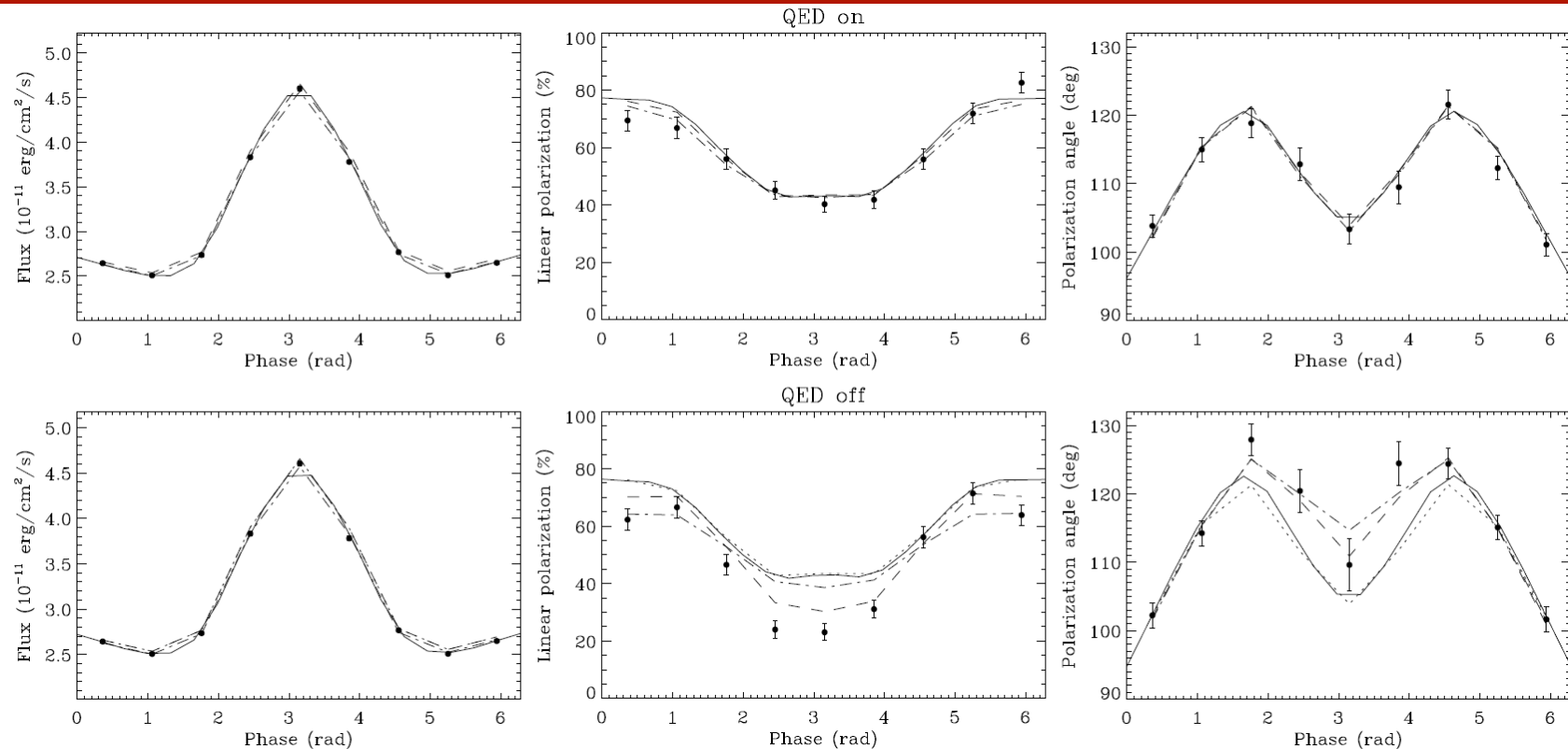


Simulated data for light curve,  $\Pi_L$  and  $\chi_{\text{pol}}$  in the QED-on and QED-off configurations, fitted by our (QED-on) theoretical model

Fit of QED-off data are not well fitted by the theoretical models

	$\beta$	$\Delta\phi_{N-S}$ (rad)	$\chi$ (deg)	$\xi$ (deg)	$\chi^2_{\text{red}}$
Input val.	0.5	1.3	90	60	—
QED-on	$0.501 \pm 0.004$	$1.17 \pm 0.03$	$90.3 \pm 1.3$	$57.9 \pm 2.2$	1.17
QED-off	$0.503 \pm 0.002$	$1.34 \pm 0.04$	$89.3 \pm 1.4$	$60.4 \pm 3.2$	7.78

# Revealing the effects of vacuum polarization



	$\beta$	$\Delta\phi_{N-S}$ (rad)	$\chi$ (deg)	$\xi$ (deg)	$\chi^2_{\text{red}}$
Input val.	0.5	1.3	90	60	—
QED-on	$0.501 \pm 0.004$	$1.17 \pm 0.03$	$90.3 \pm 1.3$	$57.9 \pm 2.2$	1.17
QED-off	$0.503 \pm 0.002$	$1.34 \pm 0.04$	$89.3 \pm 1.4$	$60.4 \pm 3.2$	7.78

## Conclusions

- Through polarization measurements one can extract the physical parameters ( $\Delta\phi_{N-S}$  and  $\beta$ ) of the source and infer with good accuracy the viewing geometry ( $\chi$  and  $\xi$  angles)
- Observations of  $\Pi_L$  and  $\chi_{pol}$  are able to remove the spectral degeneracy
- Polarimetric measures are indeed sensitive enough to reveal QED effects on the polarization observables, providing an indirect proof of the presence of a ultra-strong magnetic fields in magnetars (\*)

(\*) The first direct evidence of an ultra-strong magnetic field is quite recent:  
Tiengo et al. 2013, Nature, 500, 312

## References:

- **Taverna R., Muleri F., Turolla R. Soffitta, P., Fabiani, S., Nobili L., 2014, MNRAS 438, 1686 and other references therein**
- Bellazzini R., Muleri F., 2010, Nucl. Instrum. Methods Phys. Res. A, 623, 766
- Costa E., Soffitta P., Bellazzini R., Brez. A., Lumb N., Spandre G., 2001, Nature, 411, 662
- Fernández R., Davis S. W., 2011, ApJ, 730, 131
- Harding A. K., Lai, D., 2006, Rep. Prog. Phys., 69, 2631
- Kondratiev V. I. et al., 2009, ApJ, 702, 692
- Mereghetti S., 2008, A&AR, 15, 225
- Muleri F. et al., 2008, Nucl. Instrum. Methods Phys. Res. A, 584, 149
- Muleri F. et al., 2010, Nucl. Instrum. Methods Phys. Res. A, 620, 285
- Nobili L., Turolla R., Zane S., 2008, MNRAS, 386, 1527
- Soffitta P. et al., 2013, Exp. Astron., 36(3), 523
- Tiengo A. et al., 2013, Nature, 500, 312
- Thompson C., Lyutikov M., Kulkarni S. M., 2002 ApJ, 574, 332

Thank you for your attention!